

Phase change materials in photonic devices

Cite as: J. Appl. Phys. **129**, 030902 (2021); <https://doi.org/10.1063/5.0027868>

Submitted: 31 August 2020 . Accepted: 08 December 2020 . Published Online: 19 January 2021

 Zilun Gong, Fuyi Yang,  Letian Wang, Rui Chen, Junqiao Wu,  Costas P. Grigoropoulos, and  Jie Yao

COLLECTIONS

Paper published as part of the special topic on [Phase-Change Materials: Syntheses, Fundamentals, and Applications](#)



View Online



Export Citation



CrossMark

ARTICLES YOU MAY BE INTERESTED IN

[Acoustic subsurface-atomic force microscopy: Three-dimensional imaging at the nanoscale](#)
Journal of Applied Physics **129**, 030901 (2021); <https://doi.org/10.1063/5.0035151>

[VO₂ nanophotonics](#)

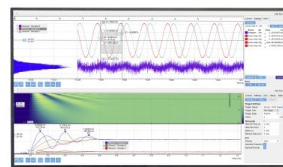
APL Photonics **5**, 110901 (2020); <https://doi.org/10.1063/5.0028093>

[Efficient mm-wave photomodulation via coupled Fabry-Perot cavities](#)

Journal of Applied Physics **129**, 033102 (2021); <https://doi.org/10.1063/5.0032506>

Challenge us.

What are your needs for
periodic signal detection?



Zurich
Instruments



Phase change materials in photonic devices

Cite as: J. Appl. Phys. 129, 030902 (2021); doi: 10.1063/5.0027868

Submitted: 31 August 2020 · Accepted: 8 December 2020 ·

Published Online: 19 January 2021



Zilun Gong,¹  Fuyi Yang,^{1,2} Letian Wang,³  Rui Chen,^{1,2} Junqiao Wu,^{1,2} Costas P. Grigoropoulos,³ 
and Jie Yao^{1,2,4,a)} 

AFFILIATIONS

¹Department of Materials Science and Engineering, University of California Berkeley, Berkeley, California 94720, USA

²Materials Sciences Division, Lawrence Berkeley National Laboratory, Berkeley, California 94720, USA

³Laser Thermal Laboratory, Department of Mechanical Engineering, University of California, Berkeley, California 94720, USA

⁴Tsinghua-Berkeley Shenzhen Institute, University of California, Berkeley, California 94720, USA

Note: This paper is part of the Special Topic on Phase-Change Materials: Syntheses, Fundamentals, and Applications.

a) Author to whom correspondence should be addressed: yaojie@berkeley.edu

ABSTRACT

Recent developments in reconfigurable photonic devices highly rely on the effective refractive index change enabled by phase change materials (PCMs) as either dielectric surroundings or constituting materials. This universal characteristic, tunable refractive index, is shared among various kinds of PCMs and has been successfully utilized to achieve multilevel modulations for both free-space and integrated photonics. In this Perspective, we briefly recapitulate the fundamental mechanisms of phase transitions for three dominant PCMs. The progress in integrating different PCMs with on-chip silicon photonics and periodic antenna arrays are reviewed and analyzed in parallel. We also discuss the existing problems of PCM photonics, for example, the compatibility with commercial production line, the stability issue, and accessibility of the stimuli. In the end, we provide the outlook for the improving material engineering of PCM and multi-functional PCM-based photonics devices.

Published under license by AIP Publishing. <https://doi.org/10.1063/5.0027868>

I. INTRODUCTION

In the interactions of light with matter, discrete electric charges in a matter are driven into oscillation by incident electromagnetic waves. Secondary radiations or scattered radiations are emitted from these accelerated charges. Each charge responds not only to the incident field but also to the secondary field generated by neighboring charges in solid-state materials. The reflection and refraction are, therefore, the superposition of secondary radiations from coupled charges. Refractive index, which depends on charge density and the polarizability of a charge, is introduced to describe the overall scattering phenomena macroscopically. Optical devices, which guide and manipulate electromagnetic wave based on diffraction and reflection, thus highly rely on the success in controlling of the refractive indices of constituting materials.

Increasing demand for better control of light propagation has led to extensive explorations on refractive index engineering. For example, different types of metamaterials have been designed to introduce sub-wavelength structures that tune the effective refractive index, usually through resonances of artificial “atoms.” In contrast to the metamaterials, one can also change the underlying

electronic structure of the material, hence modulating the refractive index. Those materials with multiple stable structural and electronic states are called phase-change materials (PCMs).² More practically, the phase of the PCMs can be controlled by parameters including temperature, electric current, strain, etc., which enables more flexible routes toward dynamic control of refractive indices. The possibility of the significant change in refractive indexes brings more degree of freedom in designing multifunctional and dynamic devices for both free space modulation and photonic integrated circuits (PICs).

PCMs typically undergo structural changes at phase transition temperatures, which result in drastic changes in the electronic structure and refractive indices.^{1,2} For example, pronounced change of electric polarizability, hence the resultant refractive index, is expected when some PCMs are transitioning from amorphous to crystalline states accompanied by the reconfiguration of chemical bonds. One can use this optical contrast in photonic devices to realize various functionalities. For example, the chalcogenide material family is successful in the applications of digital versatile disk random access memory (DVD-RAM) and Blue-ray disks.³ The

high-power laser is used to induce local phase transition by heat treatment (writing data), and then the low-power laser is used to measure the reflectance of the material (reading data). More recently, researchers have integrated the PCMs into novel platforms, such as metasurface,^{4–6} color printing,^{7–9} and integrated modulators,^{10–12} which pave the road toward broader applications of PCMs.

In this Perspective, we will review three categories of PCMs and their application in optical devices and discuss their potential developments in the future. The first category is correlated materials that are subject to Mott phase transition.¹ The vanadium oxide family, especially the vanadium dioxide (VO₂), shows metal–insulator

transition (MIT) accompanied by large refractive index change. The second category is the germanium–antimony–telluride (GST) family with fast crystalline–amorphous phase transition.³ Thanks to the resonance bonds in the metastable crystalline phase, giant optical contrast is available, which is uncommon for semiconductor materials. The third category is silicon (Si), whose (stable) crystalline FCC phase and amorphous phase show meaningful contrast in the visible frequency range.¹³ The wide applications of silicon, especially in photonics, make this relatively young direction highly attractive. We will discuss some recent advances of controlling the phase change of silicon via a pulsed laser.^{14,15} In the meantime, we will also provide some thoughts on the future research directions of those three

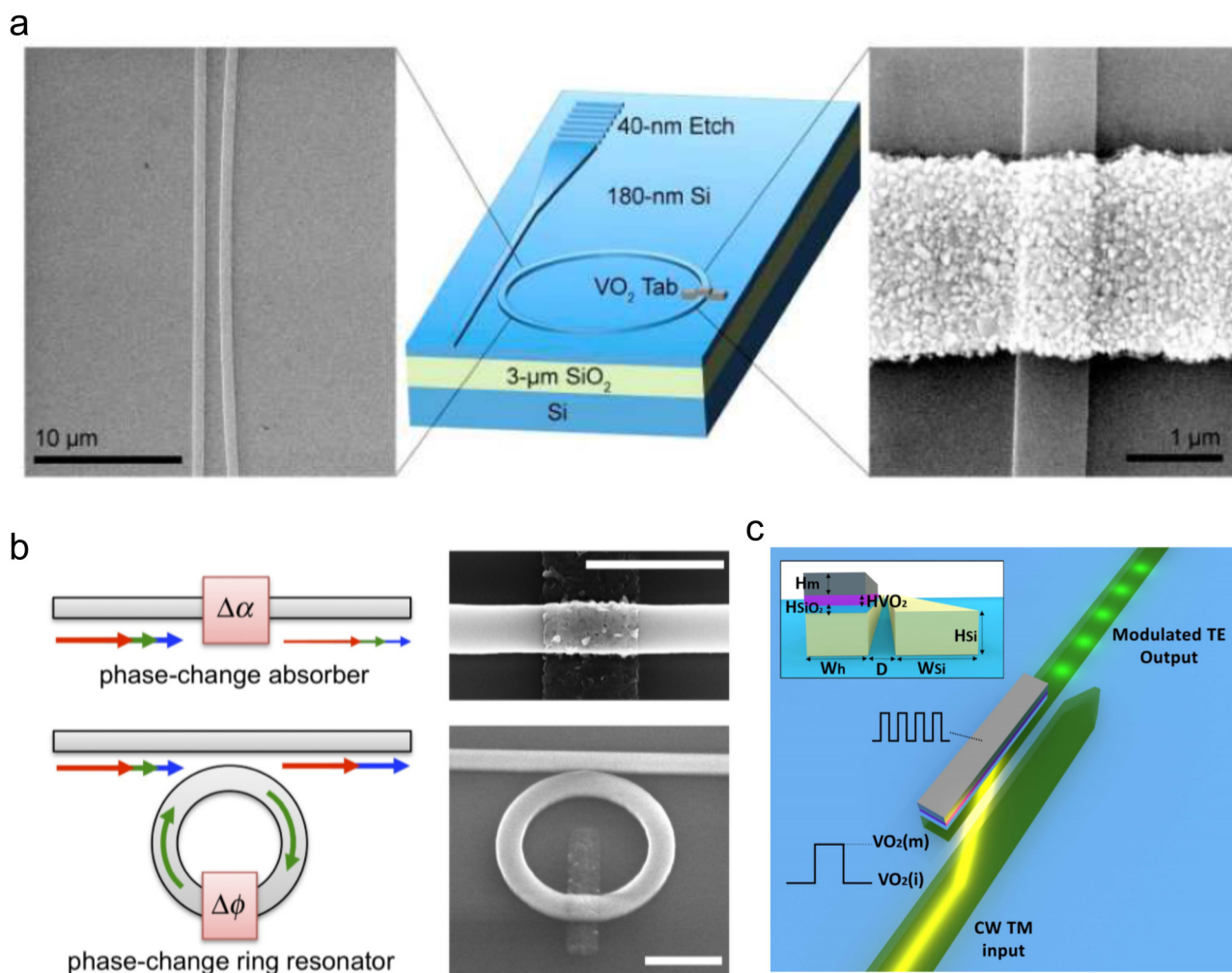


FIG. 1. VO₂ modulation in integrated photonics. (a) Schematic and SEM image of the VO₂ modulator. 2 μm-long polycrystalline VO₂ tab is deposited on the ring resonator.²¹ (b) Illustration of a phase-change absorber where MIT induces a broadband change in absorption Δα.²² (c) Schematic of electron-absorption VO₂-Si modulator with TM to TE conversion.²³ (a) Reproduced with permission from Briggs *et al.*, *Opt. Express* **18**, 11192 (2010). Copyright 2010, Optical Society of America. (b) Reproduced with permission from Ryckman *et al.*, *Opt. Express* **21**, 10753 (2013). Copyright 2013, Optical Society of America. (c) Reproduced with permission from Diana *et al.*, *J. Opt.* **19** (2017). Copyright 2017, IOP Publishing Ltd.

categories. We hope these discussions can trigger more extensive explorations of PCMs in photonic applications.

II. VO₂

Vanadium oxides are a material family known for their strong-correlation behaviors.¹⁶ Typical band structure theory is based on the single-electron approximation, where the Coulomb interactions between electrons are omitted. However, in the strong-correlation materials, the electron–electron interactions give rise to rich physics, such as Mott insulators. Mott insulators should conduct electricity under conventional band theories but show a temperature-dependent conductivity: they are insulators at low-temperature phase and conductors at high-temperature phase. This metal–insulator transition (MIT) is usually referred to as “Mott transition.”¹⁷ Vanadium dioxide, or VO₂, is a typical Mott insulator that has a phase transition temperature quite close to room temperature, at around 68 °C, making it one of the most interesting PCMs that have been explored. Applying compressive strain or doping the material with tungsten (W) can further bring down the MIT temperature.¹⁸ Accompanied with the phase transition is a large optical contrast: the relative dielectric constant is $-35 + 199i$ for the metallic phase and 4.9 for the insulating phase around 10.6 μm.^{1,19}

In its metallic phase, VO₂ has a rutile-type structure with vanadium atoms equally spaced along the corresponding *c* axis. In

its insulating phase, these vanadium atoms pair along the *c* axis with a slight twist, which leads to a monoclinic structure. Therefore, we shall refer to the two phases as R and M1, respectively. In addition, VO₂ has another monoclinic phase M2 when tensile strain is applied along the *c* axis. The phase diagram has also been developed.²⁰ In most circumstances, the insulating phase of VO₂ devices is predominantly M1 phase.

Multiple factors make VO₂ a good candidate for tunable optical devices. First, as mentioned above, the phase transition provides a large optical contrast as a function of temperature. To be specific, the M1 phase has low loss (transparent), while the R phase is very absorbing (reflective) at near to mid-infrared range.¹⁹ For example, a silicon waveguide partly covered by VO₂ film forms an optical switch upon MIT. At high temperature, when VO₂ is in the R phase and becomes very lossy, the electromagnetic field in the waveguide will be largely absorbed by the R phase and the transmission is annihilated. This idea is compatible with existing PIC devices, such as ring resonators^{21,22} [Figs. 1(a) and 1(b)] and polarization converters²³ [Fig. 1(c)]. Compact optical switches were demonstrated using the silicon-on-insulator platforms. In addition to the optical waveguide, the plasmonic waveguide can also take advantage of VO₂ with metallic structures.²⁴

VO₂ is also capable of modulating the electromagnetic wave by changing the optical modes in a periodic structure. A one-dimensional solid-state tunable Bragg filter using a VO₂ film

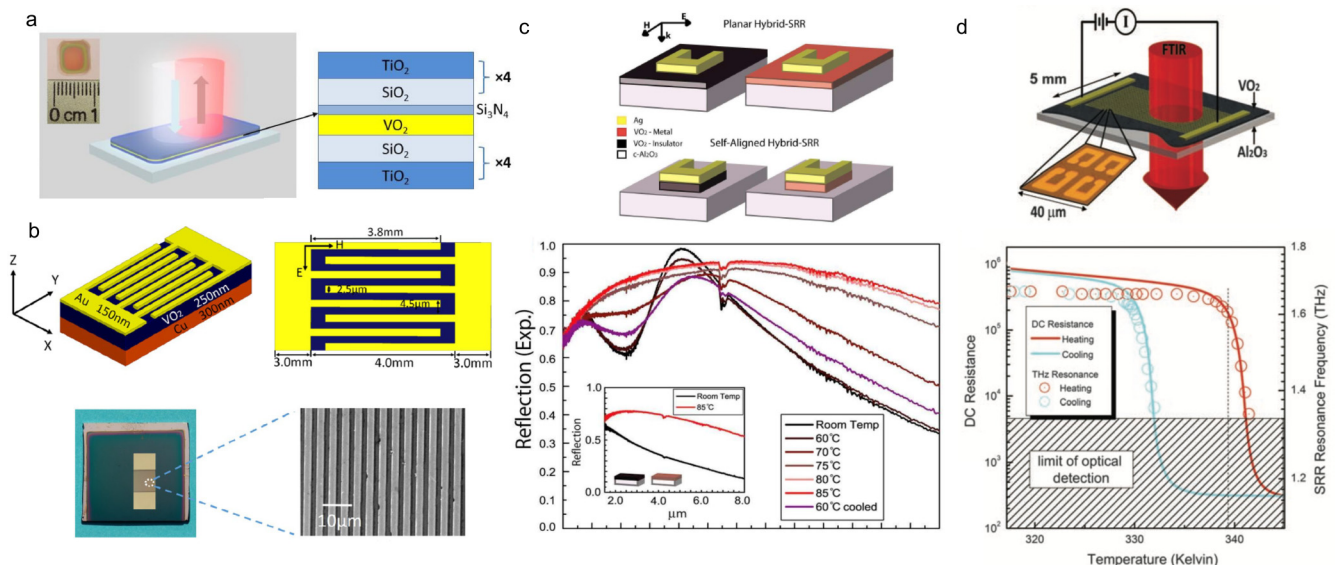


FIG. 2. VO₂ modulating free-space light with periodic structures. (a) Schematic of a tunable Bragg filter with VO₂ thin film.²⁵ (b) Schematic, optical, and SEM images of mid-infrared antenna array with a 250 nm thick VO₂ layer and a top interdigitated metal strip array.²⁶ (c) Schematic of hybrid split-ring resonator (SRR) metamaterials based on vanadium oxide.³⁰ These designs yield multiple resonances in the near-IR spectrum. As the temperature is increased above the insulator-to-metal transition temperature of VO₂, the near-IR spectral reflection properties of the SRR array become similar to those of the non-patterned metal phase VO₂ film. (d) Memory-oxide hybrid-metamaterial device with gold SRR array lithographically fabricated on VO₂ film.²⁸ Simultaneous dc-transport and far-infrared probing of the metamaterial demonstrate that as VO₂ passes through its insulator-to-metal transition, resistance drops and the SRR resonance frequency decreases. (a) Reproduced with permission from Wang *et al.*, *Opt. Express* **24**, 20365 (2016). Copyright 2016, Optical Society of America. (b) Reproduced with permission from Li *et al.*, *J. Mod. Opt.* **65**, 1809 (2018). Copyright 2018, Informa UK Limited, trading as Taylor & Francis Group. (c) Reproduced with permission from Dicken *et al.*, *Opt. Express* **17**, 18330 (2009). Copyright 2009, Optical Society of America. (d) Reproduced with permission from Driscoll *et al.*, *Science* **325**, 1518 (2009). Copyright 2013, Optical Society of America.

sandwiched between two Bragg reflectors has been demonstrated²⁵ [Fig. 2(a)]. The transparency window of the filter can be readily tuned by global heating. An electrically tunable metallic grating can be achieved by adding a layer of VO₂ film underneath it²⁶ [Fig. 2(b)]. For two-dimensional devices, VO₂ films are usually paired with an array of metallic optical antennas.^{27,28} The antennas form a 2D photonic crystal²⁹ or function as a metasurface, while the MIT of VO₂ affects or simply shifts the optical mode of these antennas^{30–33} [Figs. 2(c) and 2(d)]. It is also feasible to directly pattern antennas on VO₂ using lithography³⁴ or bottom-up synthesis,³⁵ but the finite granular feature of VO₂ makes it challenging to fabricate nanostructures with high precision.

Second, although the single-crystalline VO₂ has very little hysteresis around 1 °C in the phase transition, the deposited multi-crystalline thin film can show hysteresis with width above 10 °C. Studies have shown a correlation between the hysteresis width and grain disorientations.³⁶ A broad hysteresis makes VO₂ promising for optical storage and local phase manipulations because the same ambient temperature can host two states depending on the heat treatment.²⁸ For example, one can control the ambient temperature within the hysteresis loop and then use the laser-writing technique to raise the local temperature outside the hysteresis. As a consequence, the local optical contrast is obtained even after the local point cools down to ambient temperature. In this way, we can “write” antennas and metasurfaces on a VO₂ film and “read” the information using low-power mid-infrared light³⁷

[Figs. 3(a) and 3(b)]. Besides, the process is repeatable, meaning that patterns can be erased by global heating. Another approach for local phase control is to induce local defects from ion radiation³⁸ as shown in Fig. 3(c). The effect is similar to the local doping of W atoms, that the MIT temperature is lowered by knock off V atoms in the lattice. Within proper ambient temperature range, the devices show optical patterns defined by ion radiation [Fig. 3(d)].

Third, significant change in the VO₂ crystal lattice, thus the strain, is induced during the phase transition, which poses opportunities for optomechanical devices. Benefiting from the strain across the phase transition, VO₂-based micro-actuators are able to show giant normalized actuation amplitude with high output³⁹ [Fig. 4(a)]. Micro-cantilevers with VO₂ layer is known for good mechanical response as a function of heating^{40,41} [Fig. 4(b)]. Our group demonstrated a tunable infrared grating that the metallic grating is flat and curved when VO₂ is in metallic and insulating phases, respectively⁴² [Fig. 4(c)]. Therefore, the reflection is modulated. Note that such devices rely on the mechanical rather than optical properties of VO₂ MIT to function.

The phase transition temperature of VO₂ is relatively low and can be further lowered to room temperature with appropriate doping. Therefore, the high-temperature VO₂ R phase can be accessed thermally, electrically, or with ultrafast optical pulses. Due to the volatile nature of VO₂ transition, transient optical modulated photonic applications are supported by the VO₂ system. When thermal heating serves as the stimulus, VO₂ photonic devices have

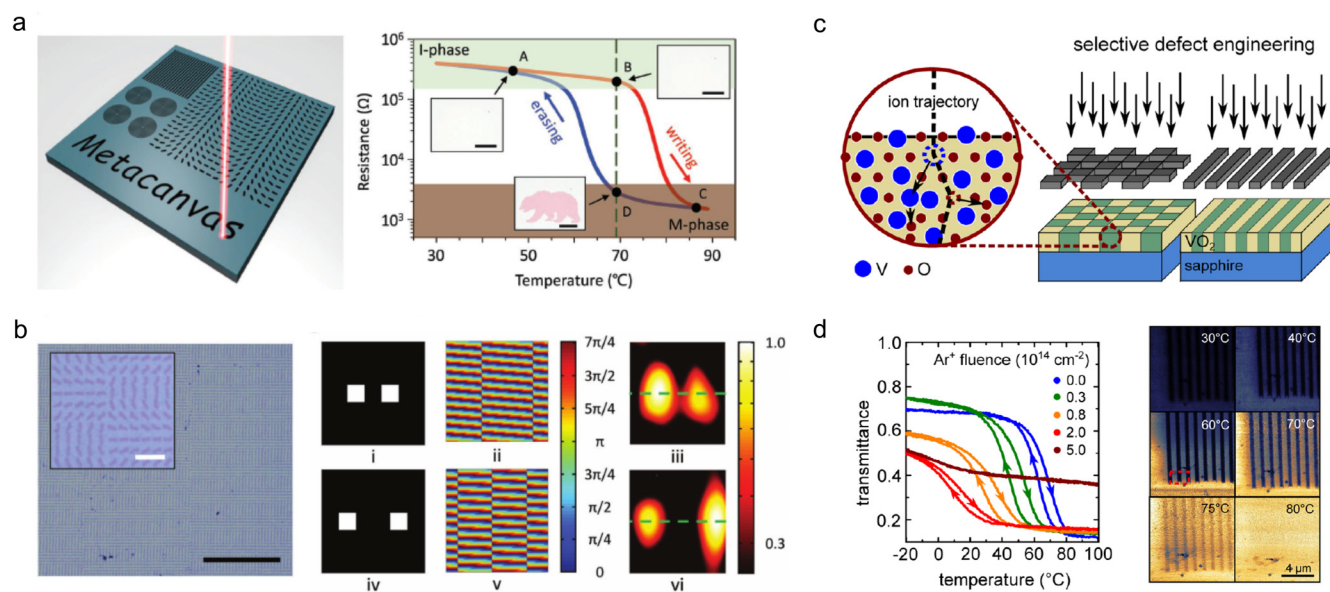


FIG. 3. Local phase manipulation of VO₂ film. (a) Schematic of laser writing different photonic operator patterns on a metacanvas³⁷ and temperature-dependent resistance of VO₂ film where the transition temperature is denoted by a vertical dashed line. (b) Optical image of a hologram compiled on the metacanvas consisting of the information of two-spot image with 18° beam steering phase distribution. Target two-spot images, corresponding phase distribution, and experimental holographic images are shown from (i) to (vi).³⁷ (c) Spatially selective defect engineering achieved by ion beam irradiation through a mask.³⁸ (d) Temperature-dependent transmittance of a 100 nm VO₂ film irradiated with Ar⁺ for various ion fluences. Contrast between the insulating and metallic phases of VO₂ is highest at intermediate temperature (~60°).³⁸ (a) and (b) Reproduced with permission from Dong *et al.*, *Adv. Mater.* **30**, 1703878 (2018). Copyright 2017, Wiley-VCH Verlag GmbH & Co. KGaA, Weinheim. (c) and (d) Reproduced with permission from Rensberg *et al.*, *Nano Lett.* **16**, 1050 (2016). Copyright 2015, American Chemical Society.

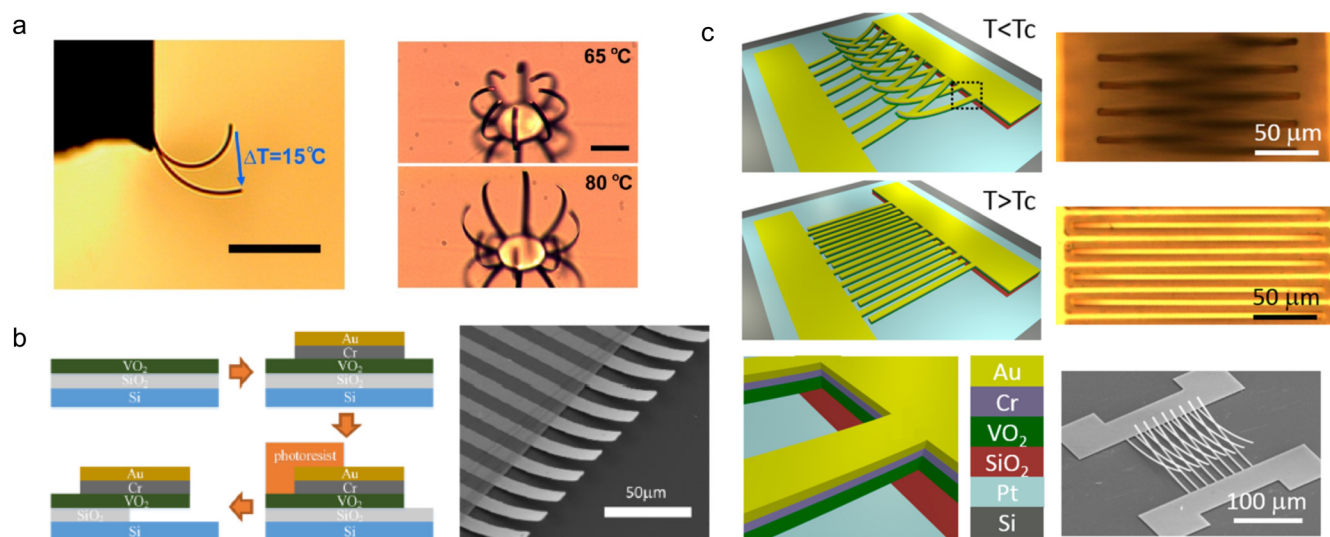


FIG. 4. VO₂ in opto-mechanical devices. (a) AVO₂ cantilevered microactuator showing a large bending amplitude when temperature is changing.³⁹ (b) VO₂ trilayer cantilever actuator design and SEM image of a released device. Temperature-dependent resistivity and cantilever deflection are also shown.⁴⁰ (c) Schematics of microelectron-opto-mechanical device with curved cantilevers at room temperature and flat cantilevers at temperature above T_c .⁴² (a) Reproduced with permission from Liu *et al.*, Nano Lett. **12**, 6302 (2012). Copyright 2012, American Chemical Society. (b) Reproduced with permission from Dong *et al.*, Appl. Phys. Lett. **109** (2016). Copyright 2016, AIP publishing LLC. (c) Reproduced with permission from Wang *et al.*, Nano Lett. **18**, 1637 (2018). Copyright 2018, American Chemical Society.

high extinction ratio and low loss, though the switching speed is inherently slow, on the order of seconds or minutes.⁴³ On the other hand, electric and optical pulses enable relatively faster switching speed around 2 ns.⁴³

A major challenge of implementing VO₂ in a practical device is its stability. A VO₂ film would quickly oxidize to V₂O₅ when exposed to air so that the devices with VO₂ film usually suffer from limited lifetime. A common way to resolve this problem is by utilizing protective layers to keep VO₂ from oxidation and deterioration. Researchers have used cladding materials to sandwich VO₂ to make a stable smart window.⁴⁵ Hydrophobic and hafnium dioxide layers have also been developed recently for encapsulation purposes, which show improved stability.⁴⁴ Successful tackling of the oxidation problem of VO₂ and reduction of production cost by low-temperature deposition methods are necessary steps toward the commercial application of VO₂-based smart windows and tunable metamaterials for long-term use.

III. GST

The family of chalcogenides hosts a variety of PCMs. Specifically, most phase change materials are found within the ternary Ge–Sb–Te (GST) phase diagram.⁴⁶ The pseudo-binary line between GeTe and Sb₂Te₃ is home to some of the most successful PCM products on the market, including the DVD-RAM and Blue-ray disk.³

A candidate material for non-volatile data storage must have two stable phases representing two distinct states with a fast transition. Besides, the two phases should have large optical contrast

because the data are accessed by the laser. The materials in the GST family typically have two stable phases at room temperature: the amorphous phase and the metastable crystalline (rock salt-type) phase. One can use different heat treatment to induce phase transitions in both ways: heating the material followed by quenching results in amorphous phase; while maintaining the temperature above the glass transition temperature for long enough time results in a crystallization phase.⁴⁷ Therefore, both phases can be manipulated and read via a focused laser, which makes the GST family ideal for data storage. Furthermore, it is possible to take advantage of the tunable refractive index and design optical devices.^{2,48}

It is generally agreed in the literature that such phase transitions in GST do not require the breaking of the chemical bond, which explains the fast transition speed.⁴⁷ At metastable rock salt phase, the Te atoms occupy one face-centered-cubic (FCC) lattice, while the Ga atoms, Sb atoms, and vacancies occupy the other FCC sublattice. For example, in Ge₂As₂Te₅, Ge and Sb atoms occupy 40% of the other FCC sublattice, respectively, while the remaining 20% sites are vacancies.⁴⁹ In the metastable phase, there are resonance bonds between short and long (nearest neighbor and next-nearest neighbor) Te–Ge bonds,⁵⁰ which explain the large index contrast (the metastable phase is more reflective than the amorphous phase). Upon excitation, the resonance bonds undergo Peierls distortion.⁵¹ The Ge atom changes from the center of a Te octahedral to the center of a Te tetrahedral.^{47,52} Once distortion occurs, it triggers the collapse of long-range order and therefore the phase transition.^{47,51}

Implementing the GST in the tunable optical devices serves a similar role as VO₂. Because both phases are stable in a wide

temperature range (including room temperature), GST has long been applied as a platform with excellent non-volatility. Here, we review some of the device demonstrations using GST, specifically $\text{Ge}_2\text{Sb}_2\text{Te}_5$ because of its low loss in the near-infrared range. For detailed discussions of metal-chalcogenide-metal (MCM) trilayered nanostructures, their design methodology, and potential challenges, there was already a very good review paper;⁴⁶ here, we mainly focus on how the GST interacts with electromagnetic waves in various photonic systems. First, GST can be used to affect the mode in the plasmonic or optical waveguides. For example, a switch is achieved when GST is applied on the waveguide or ring resonators^{53–55} [Figs. 5(a) and 5(b)]. The transmission characteristics are modulated upon phase transition. Furthermore, researchers demonstrated all-optically controlled memory: high power laser is used to write the data by heating up the GST, while the low power laser is used to read the data by measuring transmission⁵⁶ [Fig. 5(c)]. It is similar to the familiar flash memory that high and low voltages are used to write and read data, respectively. Phonon polariton-based rewritable waveguides and refractive optical elements such as metalenses have also been demonstrated by controlling the surrounding dielectric environment comprising the low-loss phase change GST.⁵⁷

Second, the GST can modulate the interaction of an electromagnetic wave with periodic structures. Most common demonstrations are using GST films with metallic antennas. Tunable absorbers with large filling ratio metallic structures^{58–60} or tunable photonic crystal showing Fano resonances⁶¹ can be made based on this concept [Figs. 6(a) and 6(b)]. In addition, GST became a

solution to the dynamic metasurface that the communities have been longing for. Both wire (bar) antennas^{62,63} and split-ring antennas^{63–65} covered by the GST film show reversible and effective optical switching behavior as shown in Fig. 6(c). Another approach is to use lithography techniques to directly fabricate antennas on the GST film without metallic structures. The one-dimensional and two-dimensional metasurfaces made of GST both have been proposed.^{6,66,67}

Third, local manipulation of phase is also feasible thanks to the laser writing and near-field probe techniques. Starting from a homogeneous GST film, focused laser can create an arbitrary pattern by induction local phase transition^{5,68} [Fig. 7(a)]. The pixel size of the pattern is determined by the focal point of laser. Sub-0.6- μm pixel size was demonstrated by a femtosecond laser.⁵ This technique also gave rise to surface phonon polariton study by creating a resonance chamber on a smooth GST film.⁶⁸

To further push down the spatial resolution, color printing was demonstrated using an atomic force microscope (AFM)^{7,8} [Fig. 7(b)]. The basic principle is to pass current locally through the GST film, and Joule heating induces phase transition. It is noteworthy that all the applications discussed except for color printing are binary: the optical memory and switches all have two states, whichever the forms are (waveguide, metasurface, etc.). However, in the more recent demonstration of color printing, gray scale was achieved. It means that one can control the percentage of phase transition locally.⁸

Accompanied with bond reconfiguration during phase transition in GST, optical loss increases significantly due to free carrier

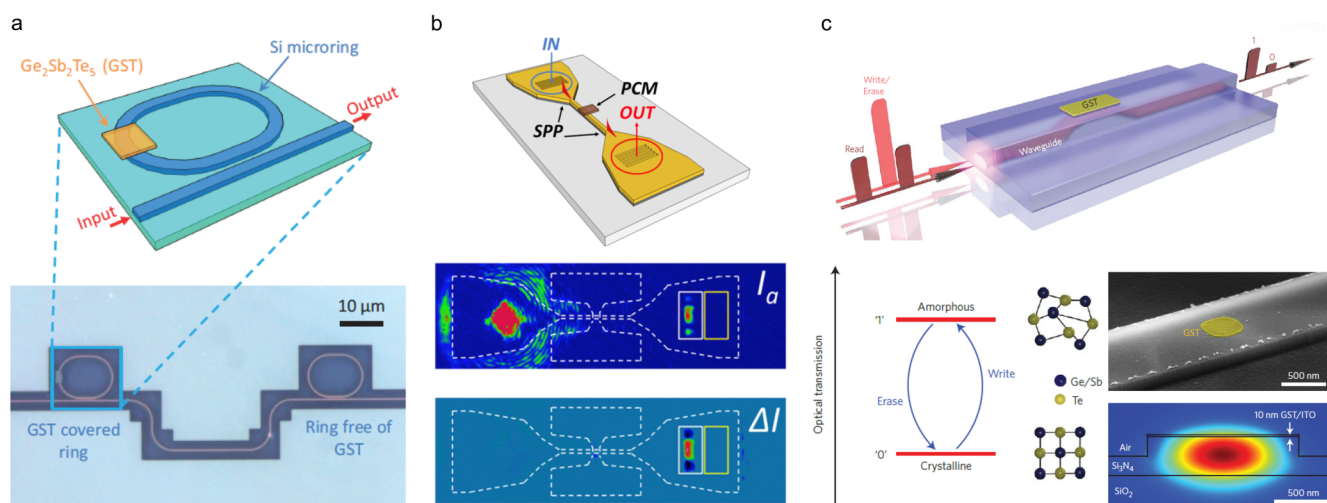


FIG. 5. GST modulation in integrated photonics. (a) An optical switch with two microrings coupled to a waveguide. One of the silicon resonators is overlaid by GST.⁵⁴ (b) Plasmonic waveguide with a GST strip in the middle. The intensity at the out-coupling grating changes strongly upon change in the GST phase, leading to a strong differential signal.⁵³ (c) An all-optical on-chip memory device with GST section on the top of the nanophotonic waveguide.⁵⁵ Less optical power is transmitted through the waveguide if the GST is in the crystalline state (level 0) than when it is in the amorphous state (level 1). TE optical mode in the waveguide evanescently couples to amorphous GST. (a) Reproduced with permission from Rudé *et al.*, *Appl. Phys. Lett.* **103**, 141119 (2013). Copyright 2013, AIP Publishing LLC. (b) Reproduced with permission from Rudé *et al.*, *ACS Photonics* **2**, 669 (2015). Copyright 2015, American Chemical Society. (c) Reproduced with permission from Ríos *et al.*, *Nat. Photonics* **9**, 725 (2015). Copyright 2016, Springer Nature.

absorption limiting their potential usage in the short wavelength range. Successful breaking of the concurrent index and loss changes based on compositionally optimized alloy Ge–Sb–Se–Te (GSST) has been shown to alleviate the loss problem by only triggering the refractive index changes without introducing loss penalty during phase transition.⁶⁹ Based on this optimized material platform, low-loss reflective pixels,⁶⁹ reconfigurable metasurface,⁷⁰ varifocal metalens,⁷¹ integrated reversible crossbar switching,⁷² and on-chip photonic multilevel memory⁷³ have been demonstrated with enhanced performances.

To further push the working frequency to the UV-visible spectral range (200–500 nm), tunable plasmonic responses of nanostructured GST are exploited.⁷⁴ The plasmon resonance due to the negative permittivity of GST in the short-wavelength range can be also considered as a design parameter for tuning the PCM-based optical devices.⁷⁵ Controllable functionalities in the UV-visible range that cannot be achieved using conventional plasmonic metals such as

optical switching, metasurface color displays, tunable perfect absorber, and performance enhancement of existing plasmonic devices.^{74,76–78}

Looking forward to further applications of GST in photonic devices, we believe the partial phase transition⁸ is promising in bringing more degree of freedom into the control. In addition, existing local phase control relies on pixel-by-pixel tuning, which is very slow. With the help of masks, it is possible to expose the whole film and speed up the formation of a pattern.

From manufacturability and quality control aspects, the chalcogenide alloys are not compatible with conventional etching and cleaning processes. Improved methods including chemical vapor deposition (CVD) and atomic layer deposition (ALD) techniques are often time-consuming and expensive. However, the developments in physical vapor deposition (PVD) and new recipes for dry etching and cleaning processes have paved the way for integrated GST photonic application.^{79,80} Several proof-of-concept demonstrations of the active GST photonic devices have been prepared on the

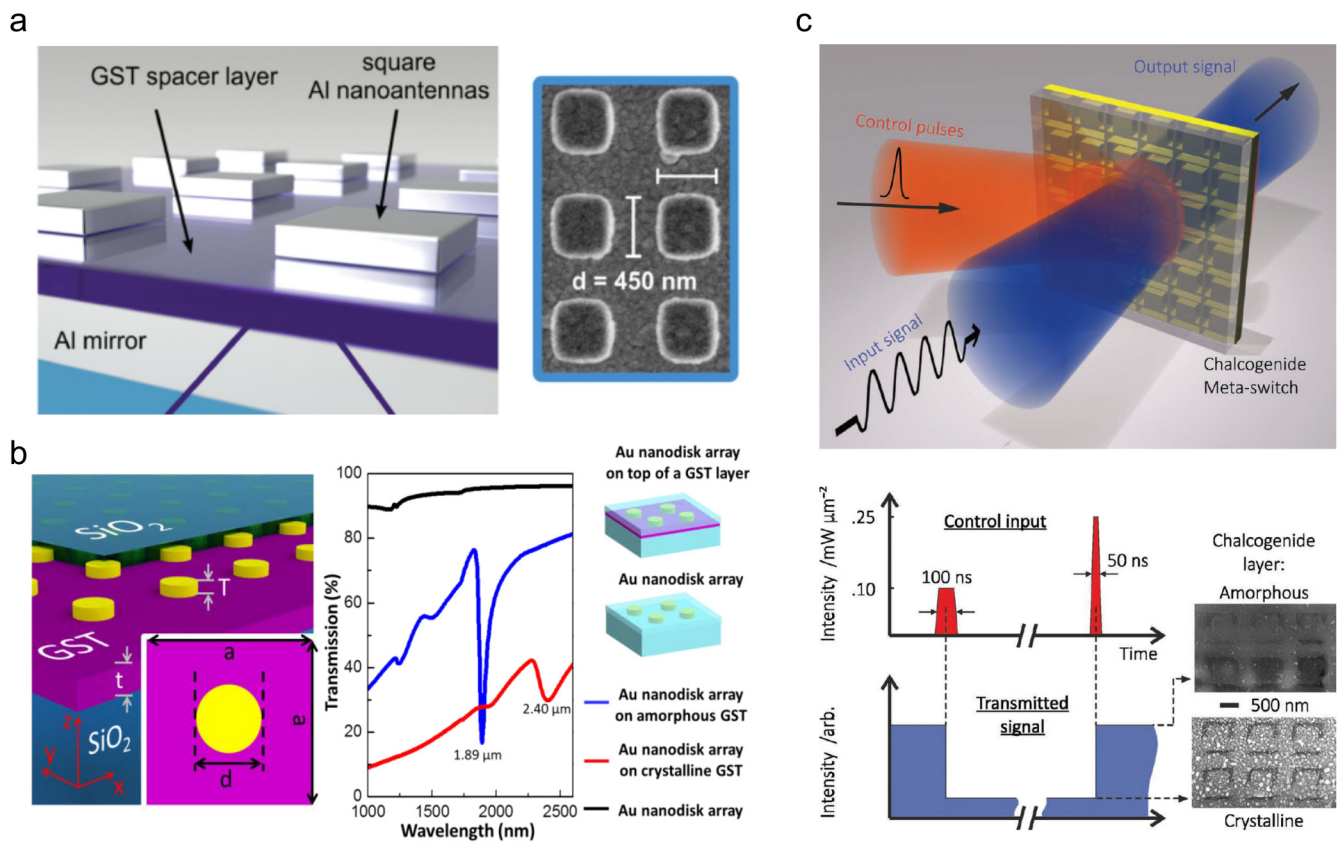


FIG. 6. GST modulating free-space light with periodic structures. (a) A switchable absorber utilizing the amorphous-to-crystalline phase transition in GST.⁵⁸ (b) Simulated transmission spectra of GST-Au hybrid plasmonic crystals with the GST layer in amorphous and crystalline phases, and a plasmonic crystal without underneath GST.⁶¹ (c) An all-optical, non-volatile, chalcogenide glass metamaterial switch that provides for high contrast transmission and reflection switching of signals at wavelengths close to the metamaterial resonances. A single laser pulse converts a chalcogenide phase-change nanolayer back and forth between amorphous and crystalline states.⁶⁵ (a) Reproduced with permission from Tittl *et al.*, *Adv. Mater.* **27**, 4597 (2015). Copyright 2015, Wiley-VCH Verlag GmbH & Co. KGaA, Weinheim. (b) Reproduced with permission from Chen *et al.*, *Opt. Express* **21**, 13691 (2013). Copyright 2013, Optical Society of America. (c) Reproduced with permission from Gholipour *et al.*, *Adv. Mater.* **25**, 3050 (2013). Copyright 2013, Wiley-VCH Verlag GmbH & Co. KGaA, Weinheim.

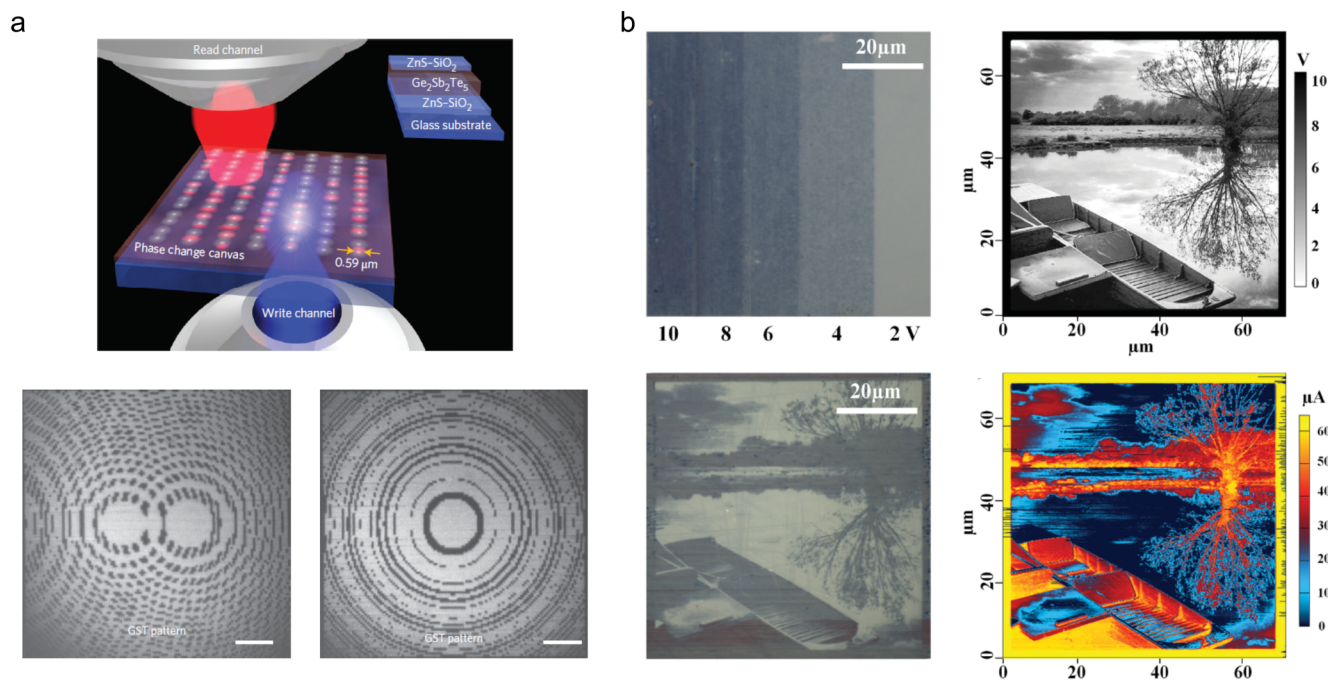


FIG. 7. Local phase manipulation on the GST film. (a) Schematic of writing reconfigurable photonic devices in GST. Optical excitation changes the complex refractive index of the film by converting continuously from the amorphous to crystalline state, allowing films with complex refractive index profiles to be written.⁵ Optical images of the lens patterns in the GST film with transverse chromatic aberration and corrected chromatic aberration are shown. (b) Grayscale images rendering and employing the GST film.⁸ (a) Reproduced with permission from Wang *et al.*, *Nat. Photonics* **10**, 60 (2016). Copyright 2015, Springer Nature. (b) Reproduced with permission from Rios *et al.*, *Adv. Mater.* **28**, 4720 (2016). Copyright 2016, Wiley-VCH Verlag GmbH & Co. KGaA, Weinheim.

CMOS compatible silicon wafer using an established method showing expected switching behavior with short switching time.^{69,81,82} Along with the progresses of compound PCMs, monoatomic phase change materials without requirement of maintaining stoichiometry during growth have also been proposed.^{13–15}

IV. Si

Silicon (Si), the ubiquitous material for the semiconductor industry and emerging photonics industry,⁸³ presents attractive features as a phase change material. From the optical performance point of view, it features high refractive index and relatively low loss in the visible wavelength range, especially the NUV range.⁸⁴ Si maintains consistent chemical composition upon repeated optical modulation. Both crystalline and amorphous resonators have been widely applied in many metasurfaces and integrated photonic devices.^{84–87} If the phase transformation and associated refractive index change of silicon itself can be utilized, the active integrated photonic device can then be readily achieved with eliminated deposition and etching steps to lower the cost and increase the yield.

Crystallinity of silicon can be easily controlled through manipulating the temperature of low-pressure chemical vapor deposition (LPCVD). Silicon's melting point could be perceived a barrier for crystallinity control; but, in fact, pulsed laser crystallization has

been well studied on thin film⁸⁸ and nanostructures.⁸⁹ The transient melting will incur minimum thermal damage to the substrate. Excimer laser annealing (ELA) has been the workhorse for the display TFT manufacturing for over a decade. The local melting is followed by slower cooling and crystallization driven by the heat diffusion to the substrate. On the other hand, if cooling is fast, pulsed laser-induced amorphization will happen on bulk materials¹⁴ and thin films.¹⁵ Studies have shown that the timescale of laser-induced silicon phase transformation varies from tens of nanoseconds⁸⁸ to sub-nanosecond⁹⁰ and, therefore, is of similar order of magnitude to current phase change materials. Hence, pulsed laser irradiation is a promising route for reversible phase change in silicon nanodomains.

Researchers recently showed that the nanosecond pulsed laser could effectively amorphize polycrystalline silicon nanoresonators of 120–300 nm in diameter.⁹¹ The difference in the crystalline and amorphous silicon's refractive indices was manifested in the switching of Mie resonances. A later report¹³ confirmed that polycrystalline and amorphous phase silicon resonators could be reversibly transformed within nanoseconds [Figs. 8(a)–8(d)]. Nanosecond laser pulses of different energies were used to transform the nanodomains with sizes down to 200 nm. These processes offered 20% non-volatile reflectance modulation, which could be repeated over 400 times. As no significant deformation was observed, the

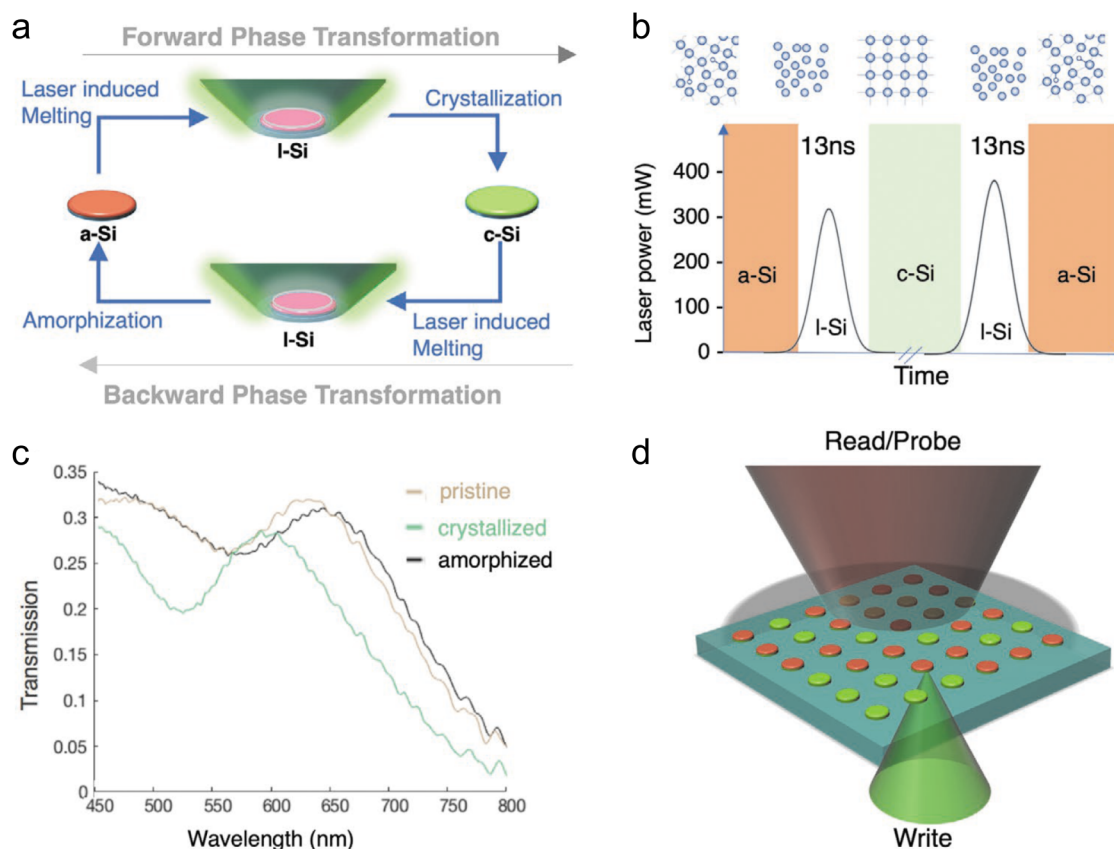


FIG. 8. Concept and application of reversible phase transformation of silicon nanostructures.¹³ (a) Schematics of reversible phase transformations of silicon nanodisks. Through laser melting the a-Si transformed to liquid and upon solidification, the material transformed to c-Si. (b) Nanosecond laser parameters used for fast reversible phase transformations of a single nanodisk. (c) Transmission spectra of pristine a-Si disks, the crystallized nanodisk, and reamorphized nanodisk with 215 nm in diameter. (d) The concept of pixel-addressable rewritable visible metasurfaces for display and optical wavefront control. (a)–(d) Reproduced with permission from Wang *et al.*, *Adv. Funct. Mater.* **1910784**, 1 (2020). Copyright 2020, Wiley-VCH Verlag GmbH & Co. KGaA, Weinheim.

resonance could be preserved, paving the way for reversible switching of photonic devices. By incorporating high N.A. laser writing,⁹² this work demonstrated a proof-of-concept experiment for dielectric display and visible wavefront control. Besides the on-demand writing, optical switching will greatly expand the device functionalities of silicon-based nanophotonics.⁸⁷ Typical applications include turning on and off Fano resonances⁹³ and edge states,⁹⁴ modifying demultiplexer functionalities,⁹⁵ and offering multilevel tunability to hybrid metamaterials.⁹⁶

For GST and silicon with high melting temperature, in order to overcome the energy barrier of the amorphous-crystalline structure, electrical and optical pulses are needed to trigger the transition. Free-space propagating optical pulses have been widely used to demonstrate GST or silicon-based tunable photonic devices. However, these devices and setups suffer from the large footprints and only suitable for free-space light modulation applications. The possibility to integrate both pump and probe optical pulses on chip, switching speed, and energy consumption will be further

improved. Along with the mature material growth capability and compatibility with CMOS technique, GST and silicon are more preferred for non-volatile integrated photonic applications.

V. Summary

Refractive index change enabled by PCMs has been utilized to achieve switching in integrated photonics, modulation of electromagnetic modes in periodic structures, and manipulation of local optical contrast. Concept demonstrations show the potential of their practical applications. However, the problems associated with the integration of the PCMs with commercial production line, the stability over time, and accessibility of the stimuli for phase transition point out the direction of research in future. The independent control of local phases will definitely bring more degree of freedom and advance the design of multi-functional devices. Better understanding and further material engineering such as doping or alloying will not only lower the transition temperature, but also allow

electric or mechanical enabled phase transitions with high integratability.

ACKNOWLEDGMENTS

This work was supported by Bakar Fellowship. J.Y. acknowledges the support from the Tsinghua-Berkeley Shenzhen Institute.

DATA AVAILABILITY

The data that support the findings of this study are available within the article.

REFERENCES

- ¹V. Eyert, *Ann. Der Phys.* **11**, 650 (2002).
- ²M. Wuttig, H. Bhaskaran, and T. Taubner, *Nat. Photonics* **11**, 465 (2017).
- ³M. Wuttig and N. Yamada, *Nat. Mater.* **6**, 824 (2007).
- ⁴H. T. Chen, A. J. Taylor, and N. Yu, *Reports Prog. Phys.* **79**, 076401 (2016).
- ⁵Q. Wang, E. T. F. Rogers, B. Gholipour, C.-M. Wang, G. Yuan, J. Teng, and N. I. Zheludev, *Nat. Photonics* **10**, 60 (2016).
- ⁶A. Karvounis, B. Gholipour, K. F. MacDonald, and N. I. Zheludev, *Appl. Phys. Lett.* **109**, 051103 (2016).
- ⁷P. Hosseini, C. D. Wright, and H. Bhaskaran, *Nature* **511**, 206 (2014).
- ⁸C. Rios, P. Hosseini, R. A. Taylor, and H. Bhaskaran, *Adv. Mater.* **28**, 4720 (2016).
- ⁹S. Yoo, T. Gwon, T. Eom, S. Kim, and C. S. Hwang, *ACS Photonics* **3**, 1265 (2016).
- ¹⁰C. Rios, P. Hosseini, C. D. Wright, H. Bhaskaran, and W. H. P. Pernice, *Adv. Mater.* **26**, 1372 (2014).
- ¹¹M. Lipson, *J. Light Technol.* **23**, 4222 (2005).
- ¹²C. Rios, M. Stegmaier, Z. Cheng, N. Youngblood, C. D. Wright, W. H. P. Pernice, and H. Bhaskaran, *Opt. Mater. Express* **8**, 2455 (2018).
- ¹³L. Wang, M. Eliceiri, Y. Deng, Y. Rho, W. Shou, H. Pan, J. Yao, and C. P. Grigoropoulos, *Adv. Funct. Mater.* **30**, 1910784 (2020).
- ¹⁴M. O. Thompson, J. W. Mayer, A. G. Cullis, H. C. Webber, N. G. Chew, J. M. Poate, and D. C. Jacobson, *Phys. Rev. Lett.* **50**, 896 (1983).
- ¹⁵T. Eiumchotchawalit and J. S. Im, *MRS Proc.* **321**, 725 (1993).
- ¹⁶C. Kittel and C.-Y. Fong, *Quantum Theory of Solids* (Wiley, New York, 1963).
- ¹⁷A. Zylbersztejn and N. F. Mott, *Phys. Rev. B* **11**, 4383 (1975).
- ¹⁸H. Takami, T. Kanki, S. Ueda, K. Kobayashi, and H. Tanaka, *Phys. Rev. B* **85**, 205111 (2012).
- ¹⁹C. Wan, Z. Zhang, D. Woolf, C. M. Hessel, J. Rensberg, J. M. Hensley, Y. Xiao, A. Shahsafi, J. Salman, S. Richter, Y. Sun, M. M. Qazilbash, R. Schmidt-Grund, C. Ronning, S. Ramanathan, and M. A. Kats, *Ann. Phys.* **531**, 1900188 (2019).
- ²⁰H. Guo, K. Chen, Y. Oh, K. Wang, C. Dejoie, S. A. Syed Asif, O. L. Warren, Z. W. Shan, J. Wu, and A. M. Minor, *Nano Lett.* **11**, 3207 (2011).
- ²¹R. M. Briggs, I. M. Pryce, and H. A. Atwater, *Opt. Express* **18**, 11192 (2010).
- ²²J. D. Ryckman, K. A. Hallman, R. E. Marvel, R. F. Haglund, and S. M. Weiss, *Opt. Express* **21**, 10753 (2013).
- ²³L. D. S. Diana, F. C. Juan, A. R. Escutia, and P. S. Kilders, *J. Opt.* **19**, 035401 (2017).
- ²⁴L. Liu, L. Kang, T. S. Mayer, and D. H. Werner, *Nat. Commun.* **7**, 13236 (2016).
- ²⁵X. Wang, Z. Gong, K. Dong, S. Lou, J. Slack, A. Anders, and J. Yao, *Opt. Express* **24**, 20365 (2016).
- ²⁶H. Li, H. Peng, C. Ji, L. Lu, Z. Li, J. Wang, Z. Wu, Y. Jiang, J. Xu, and Z. Liu, *J. Mod. Opt.* **65**, 1809 (2018).
- ²⁷L. Novotny and N. Van Hulst, *Nat. Photonics* **5**, 83 (2011).
- ²⁸T. Driscoll, H.-T. Kim, B.-G. Chae, B.-J. Kim, Y.-W. Lee, N. M. Jokerst, S. Palit, D. R. Smith, M. Di Ventra, and D. N. Basov, *Science* **325**, 1518 (2009).
- ²⁹L. Lu, J. D. Joannopoulos, and M. Soljačić, *Nat. Photonics* **8**, 821 (2014).
- ³⁰M. J. Dicken, K. Aydin, I. M. Pryce, L. A. Sweatlock, E. M. Boyd, S. Walavalkar, J. Ma, and H. A. Atwater, *Opt. Express* **17**, 18330 (2009).
- ³¹S. K. Earl, T. D. James, T. J. Davis, J. C. McCallum, R. E. Marvel, R. F. Haglund, and A. Roberts, *Opt. Express* **21**, 27503 (2013).
- ³²R. Naorem, G. Dayal, S. A. Ramakrishna, B. Rajeswaran, and A. M. Umarji, *Opt. Commun.* **346**, 154 (2015).
- ³³Z. Li, X. Wu, Z. Wu, Y. Jiang, J. Xu, and Z. Liu, *J. Mod. Opt.* **64**, 1762 (2017).
- ³⁴K. Appavoo and R. F. Haglund, *Nano Lett.* **11**, 1025 (2011).
- ³⁵T. Paik, S.-H. Hong, E. A. Gaulding, H. Caglayan, T. R. Gordon, N. Engheta, C. R. Kagan, and C. B. Murray, *ACS Nano* **8**, 797 (2014).
- ³⁶C. Petit, J.-M. Frigerio, and M. Goldmann, *J. Phys. Condens. Matter* **11**, 3259 (1999).
- ³⁷K. Dong, S. Hong, Y. Deng, H. Ma, J. Li, X. Wang, J. Yeo, L. Wang, S. Lou, K. B. Tom, K. Liu, Z. You, Y. Wei, C. P. Grigoropoulos, J. Yao, and J. Wu, *Adv. Mater.* **30**, 1703878 (2018).
- ³⁸J. Rensberg, S. Zhang, Y. Zhou, A. S. McLeod, C. Schwarz, M. Goldflam, M. Liu, J. Kerbusch, R. Nawrodt, S. Ramanathan, D. N. Basov, F. Capasso, C. Ronning, and M. A. Kats, *Nano Lett.* **16**, 1050 (2016).
- ³⁹K. Liu, C. Cheng, Z. Cheng, K. Wang, R. Ramesh, and J. Wu, *Nano Lett.* **12**, 6302 (2012).
- ⁴⁰K. Dong, S. Lou, H. S. Choe, K. Liu, Z. You, J. Yao, and J. Wu, *Appl. Phys. Lett.* **109**, 023504 (2016).
- ⁴¹K. Dong, H. S. Choe, X. Wang, H. Liu, B. Saha, C. Ko, Y. Deng, K. B. Tom, S. Lou, L. Wang, C. P. Grigoropoulos, Z. You, J. Yao, and J. Wu, *Small* **14**, 1703621 (2018).
- ⁴²X. Wang, K. Dong, H. S. Choe, H. Liu, S. Lou, K. B. Tom, H. A. Bechtel, Z. You, J. Wu, and J. Yao, *Nano Lett.* **18**, 1637 (2018).
- ⁴³K. J. Miller, R. F. Haglund, and S. M. Weiss, *Opt. Mater. Express* **8**, 2415 (2018).
- ⁴⁴T. Chang, X. Cao, N. Li, S. Long, Y. Zhu, J. Huang, H. Luo, and P. Jin, *Matter* **1**, 734 (2019).
- ⁴⁵H. Kim, Y. Kim, K. S. Kim, H. Y. Jeong, A.-R. Jang, S. H. Han, D. H. Yoon, K. S. Suh, H. S. Shin, T. Kim, and W. S. Yang, *ACS Nano* **7**, 5769 (2013).
- ⁴⁶T. Cao and M. Cen, *Adv. Theory Simulations* **2**, 1900094 (2019).
- ⁴⁷A. V. Kolobov, P. Fons, A. I. Frenkel, A. L. Ankudinov, J. Tominaga, and T. Uruga, *Nat. Mater.* **3**, 703 (2004).
- ⁴⁸J. W. Park, S. H. Eom, H. Lee, J. L. F. Da Silva, Y. S. Kang, T. Y. Lee, and Y. H. Khang, *Phys. Rev. B* **80**, 115209 (2009).
- ⁴⁹N. Yamada and T. Matsunaga, *J. Appl. Phys.* **88**, 7020 (2000).
- ⁵⁰B. Huang and J. Robertson, *Phys. Rev. B* **81**, 081204 (2010).
- ⁵¹A. V. Kolobov, M. Krbal, P. Fons, J. Tominaga, and T. Uruga, *Nat. Chem.* **3**, 311 (2011).
- ⁵²J. Hegedüs and S. R. Elliott, *Nat. Mater.* **7**, 399 (2008).
- ⁵³M. Rudé, R. E. Simpson, R. Quidant, V. Pruneri, and J. Renger, *ACS Photonics* **2**, 669 (2015).
- ⁵⁴M. Rudé, J. Pello, R. E. Simpson, J. Osmond, G. Roelkens, J. J. G. M. Van Der Tol, and V. Pruneri, *Appl. Phys. Lett.* **103**, 141119 (2013).
- ⁵⁵W. H. P. Pernice and H. Bhaskaran, *Appl. Phys. Lett.* **101**, 171101 (2012).
- ⁵⁶C. Rios, M. Stegmaier, P. Hosseini, D. Wang, T. Scherer, C. D. Wright, H. Bhaskaran, and W. H. P. Pernice, *Nat. Photonics* **9**, 725 (2015).
- ⁵⁷K. Chaudhary, M. Tamagnone, X. Yin, C. M. Spägle, S. L. Oscurato, J. Li, C. Persch, R. Li, N. A. Rubin, L. A. Jauregui, K. Watanabe, T. Taniguchi, P. Kim, M. Wuttig, J. H. Edgar, A. Ambrosio, and F. Capasso, *Nat. Commun.* **10**, 4487 (2019).
- ⁵⁸A. Tittel, A.-K. U. Michel, M. Schäferling, X. Yin, B. Gholipour, L. Cui, M. Wuttig, T. Taubner, F. Neubrech, and H. Giessen, *Adv. Mater.* **27**, 4597 (2015).
- ⁵⁹T. Cao, C. Wei, R. E. Simpson, L. Zhang, and M. J. Cryan, *Opt. Mater. Express* **3**, 1101 (2013).
- ⁶⁰T. Cao, L. Zhang, R. E. Simpson, and M. J. Cryan, *J. Opt. Soc. Am. B* **30**, 1580 (2013).
- ⁶¹Y. G. Chen, T. S. Kao, B. Ng, X. Li, X. G. Luo, B. Luk'yanchuk, S. A. Maier, and M. H. Hong, *Opt. Express* **21**, 13691 (2013).

- ⁶²A.-K. U. Michel, P. Zalden, D. N. Chigrin, M. Wuttig, A. M. Lindenberg, and T. Taubner, *ACS Photonics* **1**, 833 (2014).
- ⁶³A.-K. U. Michel, D. N. Chigrin, T. W. W. Maß, K. Schönauer, M. Salinga, M. Wuttig, and T. Taubner, *Nano Lett.* **13**, 3470 (2013).
- ⁶⁴Z. L. Samson, K. F. MacDonald, F. De Angelis, B. Gholipour, K. Knight, C. C. Huang, E. Di Fabrizio, D. W. Hewak, and N. I. Zheludev, *Appl. Phys. Lett.* **96**, 143105 (2010).
- ⁶⁵B. Gholipour, J. Zhang, K. F. MacDonald, D. W. Hewak, and N. I. Zheludev, *Adv. Mater.* **25**, 3050 (2013).
- ⁶⁶C. H. Chu, M. L. Tseng, J. Chen, P. C. Wu, Y.-H. Chen, H.-C. Wang, T.-Y. Chen, W. T. Hsieh, H. J. Wu, G. Sun, and D. P. Tsai, *Laser Photonics Rev.* **10**, 986 (2016).
- ⁶⁷L. Zou, M. Cryan, and M. Klemm, *Opt. Express* **22**, 24142 (2014).
- ⁶⁸P. Li, X. Yang, T. W. W. Maß, J. Hanss, M. Lewin, A.-K. U. Michel, M. Wuttig, and T. Taubner, *Nat. Mater.* **15**, 870 (2016).
- ⁶⁹Y. Zhang, J. B. Chou, J. Li, H. Li, Q. Du, A. Yadav, S. Zhou, M. Y. Shalaginov, Z. Fang, H. Zhong, C. Roberts, P. Robinson, B. Bohlin, C. Ríos, H. Lin, M. Kang, T. Gu, J. Warner, V. Liberman, K. Richardson, and J. Hu, *Nat. Commun.* **10**, 4279 (2019).
- ⁷⁰Y. Zhang, J. Liang, M. Shalaginov, S. Deckoff-Jones, C. Ríos, J. B. Chou, C. Roberts, S. An, C. Fowler, S. D. Campbell, B. Azhar, C. Gonçalves, K. Richardson, H. Zhang, D. H. Werner, T. Gu, and J. Hu, “Electrically reconfigurable nonvolatile metasurface using optical phase change materials,” in *2019 Proceedings Conference on Lasers Electro-Optics*, OSA Technical Digest (Optical Society of America, 2019), Paper No. JTh5B.3.
- ⁷¹M. Shalaginov, S. An, Y. Zhang, F. Yang, P. Su, V. Liberman, J. Chou, C. Roberts, M. Kang, C. Ríos, Q. Du, C. Fowler, A. Agarwal, K. Richardson, C. Rivero-Baleine, H. Zhang, J. Hu, and T. Gu, in *Conference Proceedings—Lasers and Electro-Optics Society Annual Meeting* (Proc. SPIE, 2020), Vol. 11461, Paper No. 114610M.
- ⁷²F. De Leonardi, R. Soref, V. M. N. Passaro, Y. Zhang, and J. Hu, *J. Light Technol.* **37**, 3183 (2019).
- ⁷³M. Miscuglio, J. Meng, O. Yesiliurt, Y. Zhang, L. J. Prokopenko, A. Mehrabian, J. Hu, A. V. Kildishev, and V. J. Sorger, in *2020 International Applied Computational Electromagnetics Society Symposium, Monterey, CA, 27–31 July 2020* (IEEE, 2020), pp. 1–3.
- ⁷⁴B. Gholipour, A. Karvounis, J. Yin, C. Soci, K. F. MacDonald, and N. I. Zheludev, *NPG Asia Mater.* **10**, 533 (2018).
- ⁷⁵A. K. U. Michel, M. Wuttig, and T. Taubner, *Adv. Opt. Mater.* **19**, 2549 (2017).
- ⁷⁶B. Gholipour, D. Piccinotti, A. Karvounis, K. F. Macdonald, and N. I. Zheludev, *Nano Lett.* **19**, 1643 (2019).
- ⁷⁷K. V. Sreekanth, S. Han, and R. Singh, *Adv. Mater.* **30**, 1706696 (2018).
- ⁷⁸B. Gerislioglu, G. Bakan, R. Ahuja, J. Adam, Y. K. Mishra, and A. Ahmadivand, *Mater. Today Phys.* **12**, 100178 (2020).
- ⁷⁹T. Kim, H. Choi, M. Kim, J. Yi, D. Kim, S. Cho, H. Lee, C. Hwang, E. R. Hwang, J. Song, S. Chae, Y. Chun, and J. K. Kim, in *Technical Digest—International Electron Devices Meeting (IEDM)* (IEEE, 2019).
- ⁸⁰J. D. Musgraves, N. Carlie, J. Hu, L. Petit, A. Agarwal, L. C. Kimerling, and K. A. Richardson, *Acta Mater.* **59**, 5032 (2011).
- ⁸¹J. Hu, V. Tarasov, A. Agarwal, L. Kimerling, N. Carlie, L. Petit, and K. Richardson, *Opt. Express* **15**, 2307 (2007).
- ⁸²V. Srivastava, P. Mishra, and Sunny, *Sci. Rep.* **10**, 11131 (2020).
- ⁸³B. Jalali and S. Fathpour, *J. Light Technol.* **24**, 4600 (2006).
- ⁸⁴Y. Deng, X. Wang, Z. Gong, K. Dong, S. Lou, N. Pégard, K. B. Tom, F. Yang, Z. You, L. Waller, and J. Yao, *Adv. Mater.* **30**, 1802632 (2018).
- ⁸⁵D. Lin, P. Fan, E. Hasman, and M. L. Brongersma, *Science* **345**, 298 (2014).
- ⁸⁶A. Arbabi, Y. Horie, M. Bagheri, and A. Faraon, *Nat. Nanotechnol.* **10**, 937 (2015).
- ⁸⁷I. Staude and J. Schilling, *Nat. Photonics* **11**, 274 (2017).
- ⁸⁸M. Hatano, S. Moon, M. Lee, K. Suzuki, and C. P. Grigoropoulos, *J. Appl. Phys.* **87**, 36 (2000).
- ⁸⁹B. Xiang, D. J. Hwang, J. B. In, S.-G. Ryu, J.-H. Yoo, O. Dubon, A. M. Minor, and C. P. Grigoropoulos, *Nano Lett.* **12**, 2524 (2012).
- ⁹⁰Y. Izawa, S. Tokita, M. Fujita, M. Nakai, T. Norimatsu, and Y. Izawa, *J. Appl. Phys.* **105**, 064909 (2009).
- ⁹¹L. Wang, Y. Rho, W. Shou, S. Hong, K. Kato, M. Eliceiri, M. Shi, C. P. Grigoropoulos, H. Pan, C. Carraro, and D. Qi, *ACS Nano* **12**, 2231 (2018).
- ⁹²X. Zhu, W. Yan, U. Levy, N. A. Mortensen, and A. Kristensen, *Sci. Adv.* **3**, e1602487 (2017).
- ⁹³K. E. Chong, B. Hopkins, I. Staude, A. E. Miroshnichenko, J. Dominguez, M. Decker, D. N. Neshev, I. Brener, and Y. S. Kivshar, *Small* **10**, 1985 (2014).
- ⁹⁴S. Kruk, A. Slobozhanyuk, D. Denkova, A. Poddubny, I. Kravchenko, A. Miroshnichenko, D. Neshev, and Y. Kivshar, *Small* **13**, 1603190 (2017).
- ⁹⁵A. Y. Piggott, J. Lu, K. G. Lagoudakis, J. Petykiewicz, T. M. Babinec, and J. Vučković, *Nat. Photonics* **9**, 374 (2015).
- ⁹⁶C. R. de Galarreta, I. Sinev, A. M. Alexeev, P. Trofimov, K. Ladutenko, S. G.-C. Carrillo, E. Gemo, A. Baldycheva, V. K. Nagareddy, J. Bertolotti, and C. D. Wright, *arXiv:1901.04955* (2019).